INVESTIGATING THE SPATIAL DISTRIBUTION OF SMALL RAYED CRATERS ON MARS: HOW LONG DO THEY RETAIN THEIR RAYS? F. J. Calef III[1], V. L. Sharpton[1,2] and R. Herrick[2], [1]Department of Geology and Geophysics, University of Alaska, Fairbanks, AK, 99739, fred@gi.alaska.edu, [2]Geophysical Institute, University of Alaska, Fairbanks, AK, 99739, buck.sharpton@alaska.edu, rherrick@gi.alaska.edu.

Introduction: Mars crater production functions, instrumental in generating absolute dates of planetary surfaces and geologic events, rely upon an accurate estimate of the impactor flux [1,2]. A recent study has recorded the current martian impactor flux at 1.35 x10^{-7}craters/km^2/yr (20 craters/21.5x10^6km^2/6.85 years) by observing new rayed craters (diameters <200m) formed in the dusty Amazonis/Tharsis (A/T) and Arabia regions [3]. Previous research indicated a population of rayed craters, <1km in diameter, whose ejecta varied in albedo and spatial extent [4]. Our current research presented here focuses on the global distribution of small (<1km diameter) rayed craters, their associated ejecta retention time and mechanisms, and discerning primary versus secondary craters in this population. We compare our findings from a global random sampling of Mars Orbiter Camera Narrow Angle (MOCNA) imagery for rayed craters to the above study to better estimate the global ejecta retention rate. We will also discuss if secondary crater 'contamination' from several large primaries is prevalent.

Methodology: We selected a 5% random sample of MOCNA images up to mapping subphase S10. No bias was given to image pixel size or areal extent given that these parameters should balance each other out; images with large footprints will have a greater pixel size and chance to find rayed craters, but will be limited to larger (~>75m) craters in the sub-kilometer diameter range, while small image footprints with smaller pixel sizes will find more small (~<75m) diameter craters, but less of them. We evaluated the MOCNA footprint ability to sample the martian surface by comparing the area covered by the footprints to both the elevation and age unit global distribution. Both the elevation and age units for Mars were sampled within the standard error by our sample. This gives us confidence that our image sample is representative of the global martian surface despite the fact that MOCNA images are targeted and non-random at the global scale. For comparison, we clipped the sample by the boundaries defined by [3] and counted all <200m diameter rayed craters. We then calculated a retention age by setting our sample area and crater counts equal to the cratering rate from [3]:

$$Age_{SR} = (A_T/A_S)*(C_S/C_T)*Age_{TR}$$

where Age_{SR} is our (sample) retention age, A_T is the total area studied in [3], A_S is our sample study area, C_S is total rayed craters in our sample, C_T is the total number of craters from [3], and Age_{TR} is the time period covered by [3]. This formula is most sensitive to the crater counts, so we estimate ~10% error in our sample. Retention ages were generated for the total, A/T, and Arabia study areas as defined by [3].

Maximum Secondary Crater Range: To evaluate the potential for secondary craters occurring within our global population, we used an analytical ballistic formula [5] to generate maximum ellipses from the centroids of eight known primary craters [6] and used the maximum ray distances observed as these areas represent heavy concentrations of secondary craters associated with ray generation [6].

Ignoring atmospheric friction, the maximum range a secondary could travel from a primary was calculated using:

$$R_S=2R_p\tan^{-1}[((v_e^2/R_Pg)\sin\theta\cos\theta)/(1-(v_e^2/R_Pg)\cos^2\theta)]$$

where secondary range (R_S) from impact is a simple function of the planet's radius (R_P), gravity (g), ejection velocity (v_e) and ejection angle (θ). If the secondary approached escape velocity (5km/s), assuming a 45º launch angle and no interference from the atmosphere, R_S would be ~10500km. We used this value and the maximum ray length to map a radial area around each primary to determine which small rayed craters, under this 'best case' model, occurred within the secondary range.

Results: From the global sample of 4264 images, 227 (5.3%) were determined to have small rayed craters. Of this global sample, 444 images fell within the [3] study area, with 31 (7%) containing small rayed craters. Our image sample area (3.85x10^4km^2 cumulative) in the two study regions is within 1% of the ratio of surface areas delineated; 66% in A/T (14.3x10^6km^2) and 33% in Arabia (7.2x10^6km^2) of a total 21.5x10^6km^2. A total of 101 rayed craters <200m in diameter were identified. However, the A/T region recorded only 18 craters compared to 83 identified in Arabia within our sample. Two images (E13/00423 and M08/01879) within Arabia recorded 20 and 29 craters respectively, while other images recorded 1-4 craters/image. For the purposes of this research, we exclude counts from these two anomalous images in our calculations. All rayed craters in these two images are well preserved with distinct rays of varying albedo (i.e. dark and/or bright) with no infilling. These images

may represent areas of increased preservation (i.e. low dust deposition and decreased wind erosion), a large meteorite breakup, or secondaries from an undiscovered primary (to be discussed). Given the above caveat, each image contains ~2 craters. There is a 1:1.9 (18/34) difference in crater counts between the two areas despite a reverse 2:1 ratio in areal extent. This stands in stark contrast to the 13 new craters in A/T and 7 in Arabia reported by [3]. Using our retention age formula with a total of 52 craters, we calculated the following retention values:

Age_{Total}:	10,000 years
$Age_{Tharsis}$:	5,200 years
Age_{Arabia}:	19,000 years

for the total study area in [3], A/T and Arabia, respectively. Based on ~10% error in the crater counting, all retention ages are ±1000 years.

Looking at the secondary ellipses from known rayed primaries (Figure 1), given that rayed craters are younger than non-rayed craters in a given size range, no study region is beyond the maximum extent of all secondary crater formation. While A/T is ~75% covered by all eight secondary crater ellipses, two cover ~40% and five cover ~60% of Arabia. Given the low crater count in A/T, we see no significant secondary crater contamination. Although there are more craters in Arabia, fewer secondary ellipses cross this region, also suggesting low contamination, except perhaps the two anomalous images. In comparison, the ellipses generated by primary crater ray length cover only ~1/3 of the western edge of A/T and a small southern section. Given that many secondaries are clustered within the rays, we are confident that secondary contamination is minimal across most of Mars from these rayed primaries.

Discussion: Ejecta retention on Mars must be a function of either the crater target (i.e. the material properties of the impacted geologic formation), the surface environment (i.e. erosional and depositional processes) or both. There is evidence that both play significant roles. If we look at the global distribution of rayed craters (Figure 1), there are obvious paucities of craters in the erosionally active polar regions; areas known for dust devils, dune fields (migration?), and thermokarst activity. Retention mechanisms in other regions on Mars are not so easy to deduce. Comparing our global study to the distribution of water equivalent hydrogen (WEH) [7], the number of images with rayed craters increases with higher %WEH values (Figure 1). The Arabia region has overall greater %WEH values than A/T. Our initial results indicate %WEH correlates with increased ejecta retention.

Secondary craters could skew our results if there are significant quantities within the study region. Given that A/T has a factor of 2 times fewer rayed craters than Arabia, and Arabia falls under fewer secondary crater ellipses, there is limited suggestion that secondary craters contaminate our study. At most, a global study must exclude only those areas immediately near or within the rays of known large primaries. Given those stipulations, our global sampling of rayed craters does not appear to be significantly biased by secondary crater formation.

Conclusion: Overall, our results suggest a retention age for small rayed craters on the order of 10,000 ±1000 years. Rays around small craters are clearly much more persistent albedo features than dust devil tracks or slope streaks whose retention age is perhaps seasonal [8] and decadal [9] rather than millennial. Obvious regional variations in retention ages exist, yet it is evident that the 'weathering' (i.e. erosion and deposition) mechanisms necessary to remove these rays must be more extensive than a few global atmospheric events.

Future Work: We are in the process of quantifying the %WEH correlation to the global small rayed crater population as well as investigating secondary cratering distances using a numerical deterministic atmospheric friction model.

References: [1] Hartmann W. K. et al. (2001) *Icarus*, 149. [2] Hartmann W. K. (2005) *Icarus*, 174. [3] Malin et al. (2006) *Science*, *314*, 1573-1577. [4] Calef F. J. III et al. (2004) *Fall AGU*, no. P41A-0890. [5] Ahrens T. J. and O'Keefe J. D. (1978) *LPSC IX*, pp. 3787-3802. [6] Tornabene et al. (2006) *JGR*, *111*, 2005JE002600. [7] Felman et al., (2004) *GRL*, *109*, 2003JE002160. [8] Balme et al., (2003) *JGR*, *108*, 2003JE002096. [9] Aharonson et al., (2003) *JGR*, *108*, 2003JE002123.

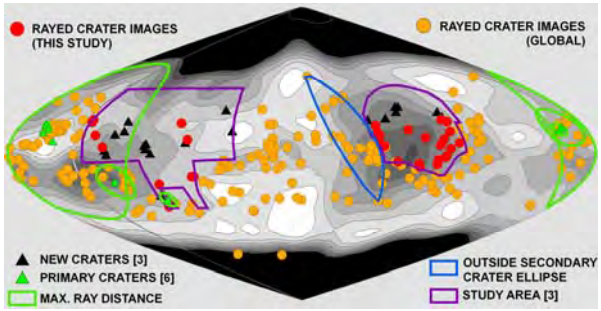

Figure 1: Map of rayed crater image locations and possible secondary ellipses. %WEH from [7]; white = 3% to dark grey = 10%, black = >10%. Sinusoidal projection centered at 40°W. Study regions in purple; Amazonis/Tharsis (A/T) on left, Arabia on right.